Figures S1: Analysis of the interaction between CpsD and Spr0895 (RocS)

(**A**) Protein-protein interaction between CpsD and RocS (Spr0895) assayed by yeast two-hybrid. AD and BD refer to activating and DNA binding domain of Gal4 fused to either CpsD, $RocS_{(50-163)}$, $RocS_{(1-163)}$, or CpsC, and CpsD, respectively. The Spr0895 minimal interacting domain necessary for interaction with CpsD was delineated from residue 50 to 163. Protein-protein interactions were assayed by the ability of the diploids to grow on SC-LUH selective media (without histidine). (-) indicates empty vectors, used as negative controls. Interaction between BD-CpsD and AD-CpsC or AD-CpsD were used as positive controls as previously reported (*10*). (**B**) Protein purification. The chimera CpsC/D and RocS-ΔAH (RocS devoid of the C-terminal amphipatic helix, see Fig. S10) were overproduced in *E. coli* as 6His-tagged fusion proteins. After purification using a Ni-NTA resin, 6His-CpsC/D and RocS-ΔAH-6His were analyzed by SDS-PAGE. (**C**) Affinity measurements by Microscale Thermophoresis of labeled RocS binding to increasing concentrations of 6His-CpsC/D chimera. FNorm (normalized fluorescence) is plotted as a function of ligand concentration. Measurements are represented by blue dots and the fitted curve by a green line. Three independent experiments were performed.

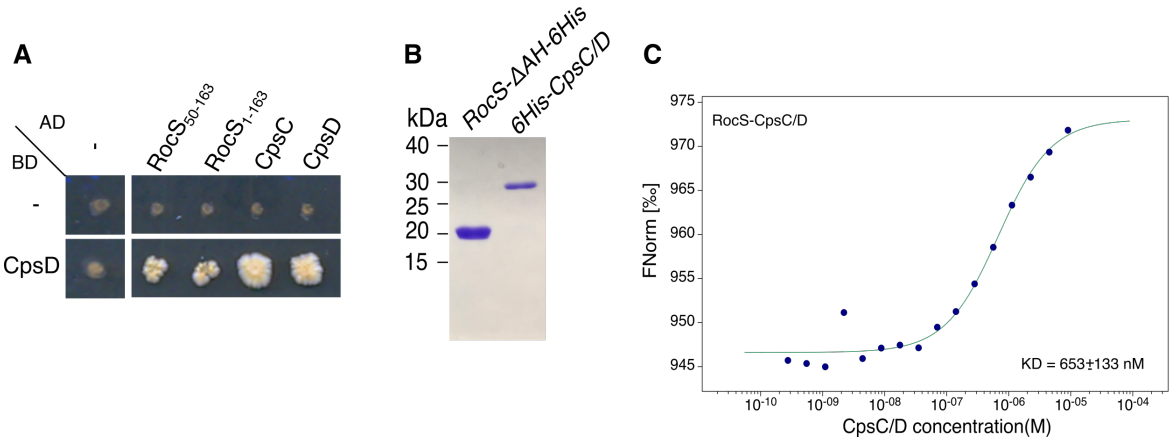

Figure S2: Taxonomic distribution of RocS in *Lactobacillales*.

The number of species containing a RocS homolog compared with the total number of sequenced species in the genera are indicated. The relative proportion of genomes containing at least one copy of *rocS* are color coded using a green scale.

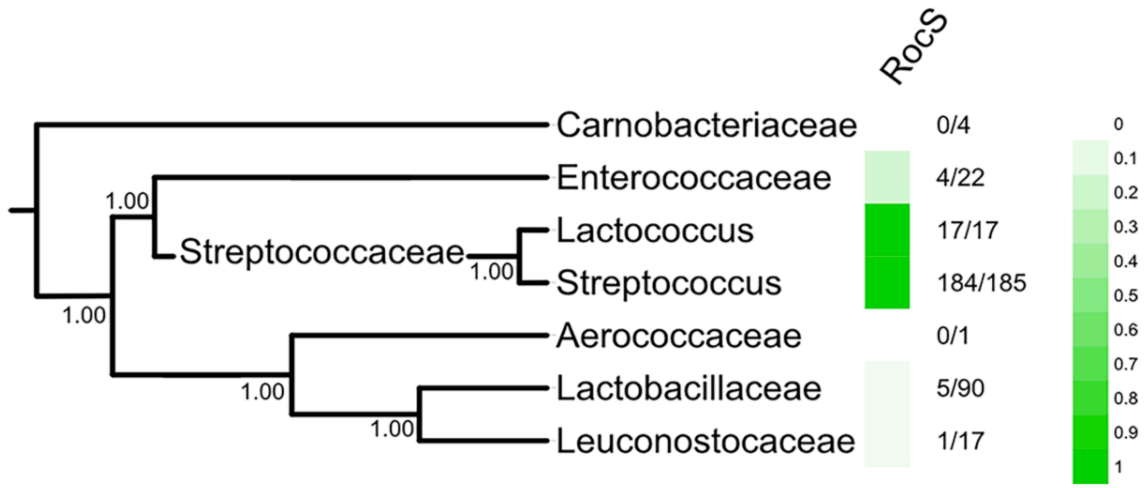

Figure S3: Production of capsular polysaccharides (CPS)
Detection of cell-associated CPS in the D39 strain and the Δ*cpsD* and Δ*rocS* derivatives. The same volume of CPS prepared from culture grown until OD_{550} = 0.3 was loaded in each lane. The immunoblot was probed with a rabbit anti-serotype 2 CPS polyclonal antibody.

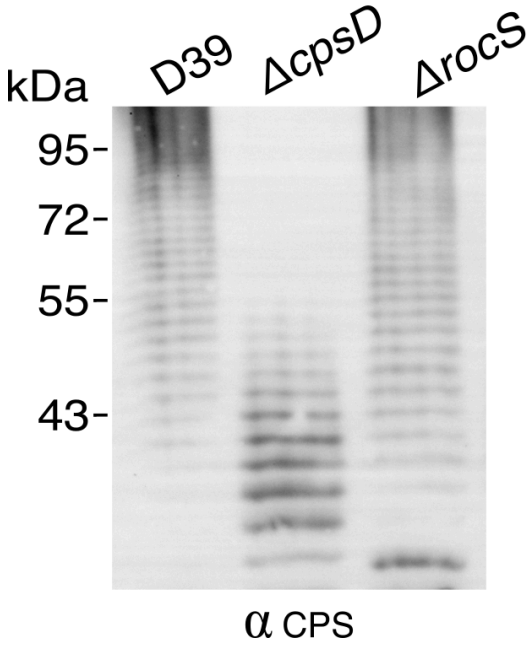

Figure S4: Growth and cell shape analysis of D39 and Δ*rocS* strains

(**A**) Representative growth curves for the D39 strain and the Δ*rocS* derivative. Strains were grown in CH+Y medium at 37 °C in a JASCO V-630 Biospectrophotometer. The OD_{550} was read automatically every 10 min. Shown curves are representative of three replicates. GT is for generation time. (**B-C**) Cell length (B) and width (C) distribution of D39 and Δ*rocS* cells. n_T indicates the total number of cells analyzed from three independent experiments.

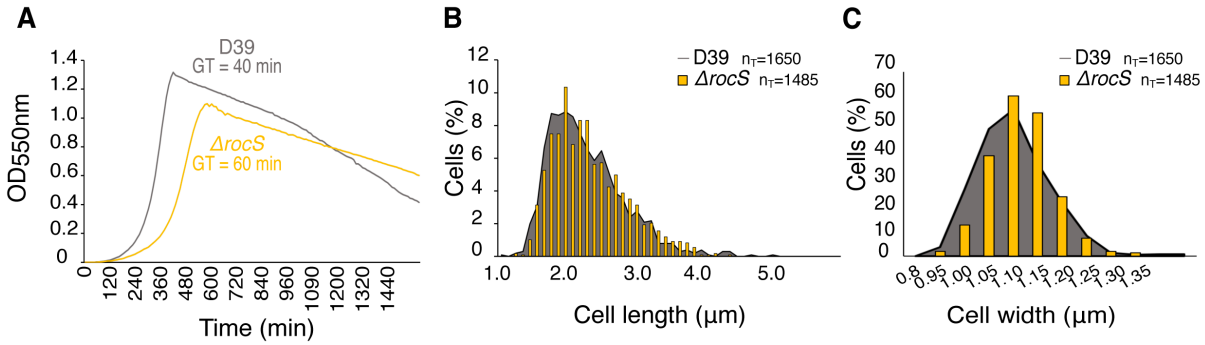

Figure S5: Impact of *rocS* deletion on nucleoid distribution, cell-growth and -shape of R800 cells

(**A**) Visualization of nucleoids in the R800 strain and the Δ*rocS* derivative. Localization of nucleoids was analyzed using DAPI staining. Phase contrast (left column) and overlays between phase contrast and DAPI fluorescent signal (right column). Arrowheads indicate anucleate cells. Scale bar, 1 µm. (**B**) Representative growth curves for the R800 strain, the Δ*rocS* derivative and the complementation strain. Strains were grown in CH+Y medium at 37 °C in a JASCO V-630 Biospectrophotometer. The OD_{550} was read automatically every 10 min. They are representative of three replicates. GT is for generation time. (**C-D**) Cell length (C) and width (D) distribution of R800 and Δ*rocS* cells. n_T indicates the total number of cells analyzed. Experiments were performed in triplicates.

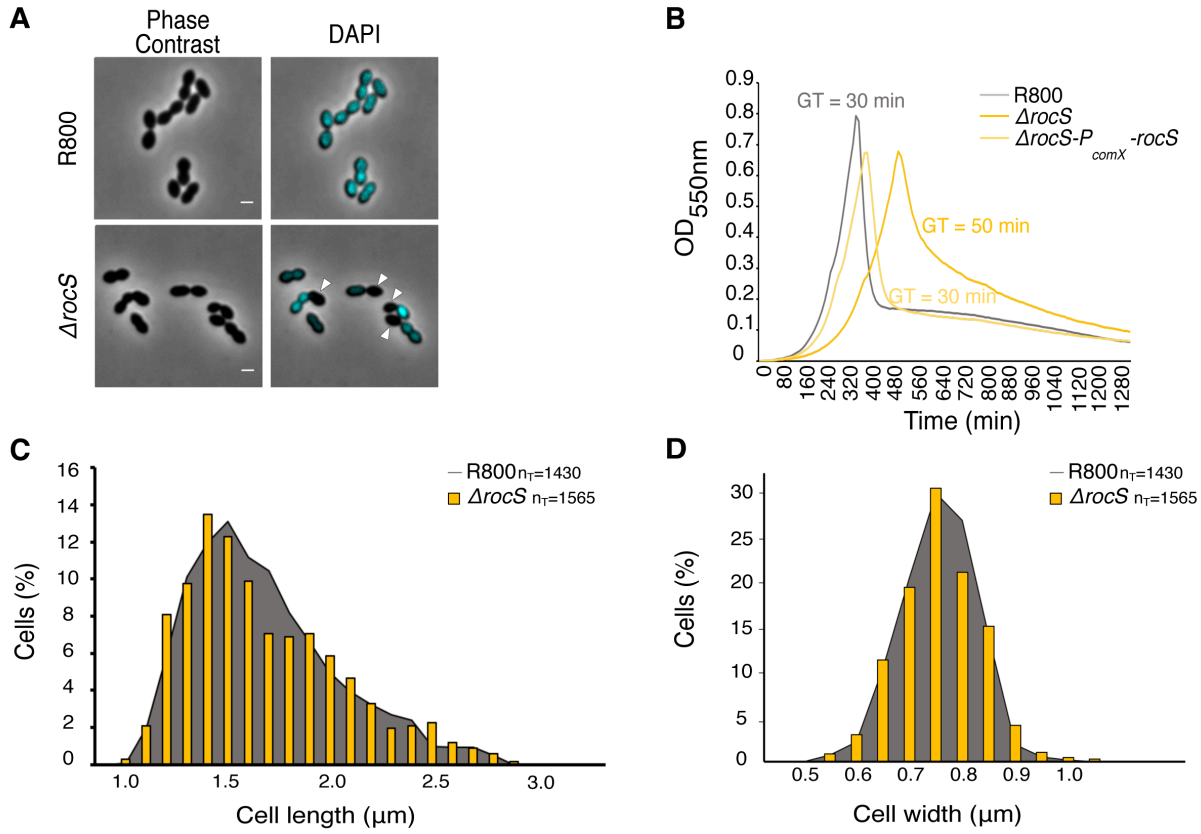

Figure S6: Marker frequency analysis of the *oriC* and *ter* regions
Boxplot representing the ratio between the origin of replication (*oriC*) and the terminus region (*ter*) of the chromosome determined by real-time qPCR of chromosomal DNA isolated from exponentially growing Δ*rocS* and Δ*rocS*-P_{comX}*rocS* cells. As controls, the *oriC*/*ter* ratio was determined for R800 cells and for a thermo-sensitive *dnaA-T1193C*(M398T) mutant (TS). Whiskers represent the 10th and the 90th percentile of data from Monte Carlo simulations.

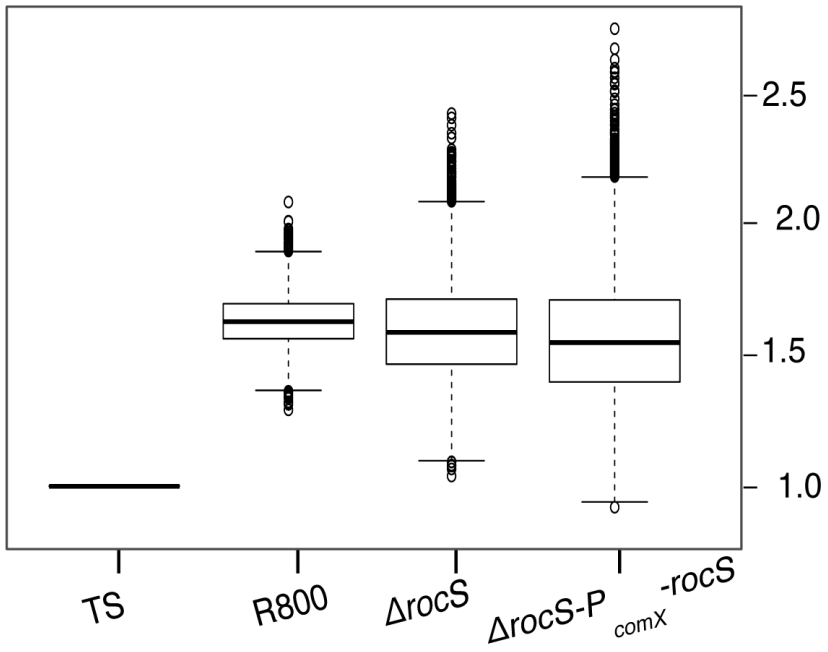

Figure S7: Validation of strains expressing the *ori* localization system
Representative growth curves for the R800 strain and P_{comX}-*repC-gfp*, $parS_{Ef}$ and $parS_{Ef}$-P_{comX}-*repC-gfp* derivatives. Strains were grown in CH+Y medium at 37 °C in a JASCO V-630 Biospectrophotometer. The OD_{550} was read automatically every 10 min. Curves are representative of three replicates. Overlays between phase contrast and GFP fluorescence signal are shown on the right to illustrate that the cell shape is not affected and that RepC-GFP localizes either in the cytoplasm or as 2 bright foci in the absence or presence of $parS_{Ef}$ sites, respectively.

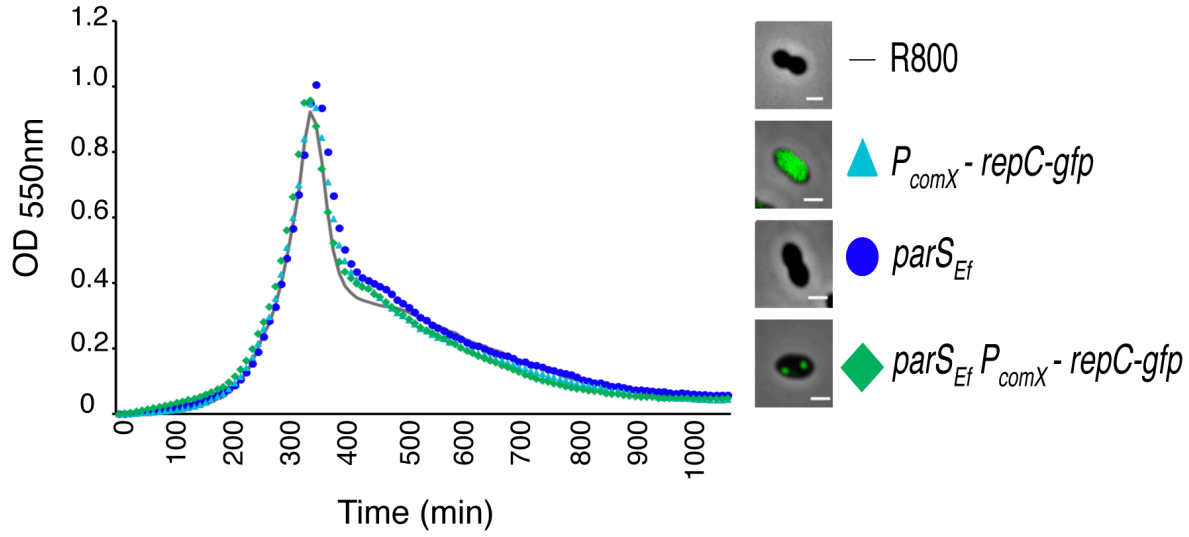

Figure S8: Growth curves and nucleoid distribution of cells producing GFP and Flag fusions.

(**A**) Growth curves of R800 (grey) and Δ*rocS* cells (orange) and cells expressing either *gfp-rocS* (dark blue) or *gfp-rocS-ΔAH* (light blue) or *gfp-ΔHTH-rocS* (light orange) or *flag-rocS* (light grey) in CH+Y medium at 37 °C. The OD550 was read automatically every 10 min. All fusion proteins are the only source of RocS, RocS-ΔAH and ΔHTH-RocS in cells. The fusion genes encoding these proteins substitute the corresponding native genes at their chromosomal locus. (**B**) Percentage of anucleate cells in R800, Δ*rocS* and *gfp-rocS* strains. n_T indicates the number of cells analyzed from n=3 independent experiments and standard errors are indicated with error bars. (Two population proportions test: ****P<0.0001).

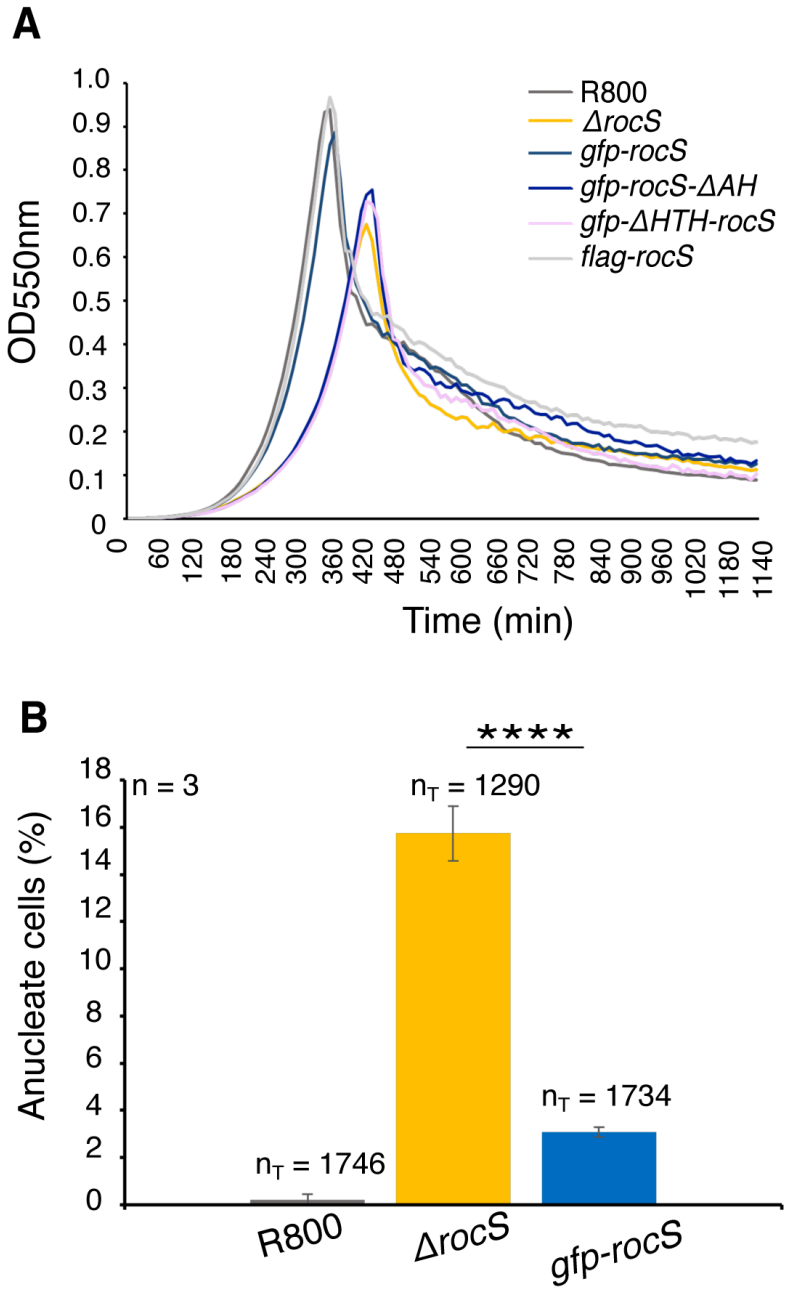

Figure S9: Expression of *rocS* fusions

The Western immunoblot was probed with specific anti-RocS antibodies (α RocS) to determine *rocS* expression in R800, *gfp-rocS*, *gfp-rocS-ΔAH*, *gfp-ΔHTH-rocS* and *flag-rocS* cells. To estimate the relative quantity of proteins in crude extract and to compare the different lanes, we used enolase (Spr1036) as an internal standard. The enolase was detected using specific antibodies (α Enolase) as described in (*23*) and is presented in the lower part of the figure.

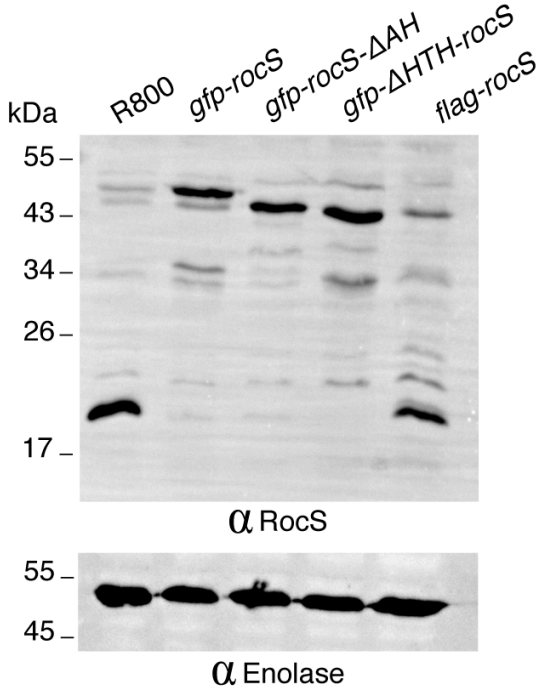

Figure S10: Bioinformatic analysis of the amino acid sequence of RocS
(**A**) Secondary structure prediction of RocS using PSIPRED (*40*). The prediction of an N-terminal Helix-Turn-Helix domain (HTH) and a C-terminal amphipathic helix (AH) is shown in blue and green, respectively. a, b and c show the predicted secondary structure, the confidence of prediction and the RocS sequence, respectively. (**B**) Drawing of RocS with the N-terminal Helix-Turn-Helix in blue and the C-terminal amphipathic helix in green. The central predicted α-helix is shown in grey. Sequence alignment and helical representation of the amphipatic helices of RocS and MinD of *E. coli* (*19*) are shown on the right. Non-polar residues are shown in green. The dotted-lines show that the composition of the upper-side of each helix is amenable to interacting with the membrane.

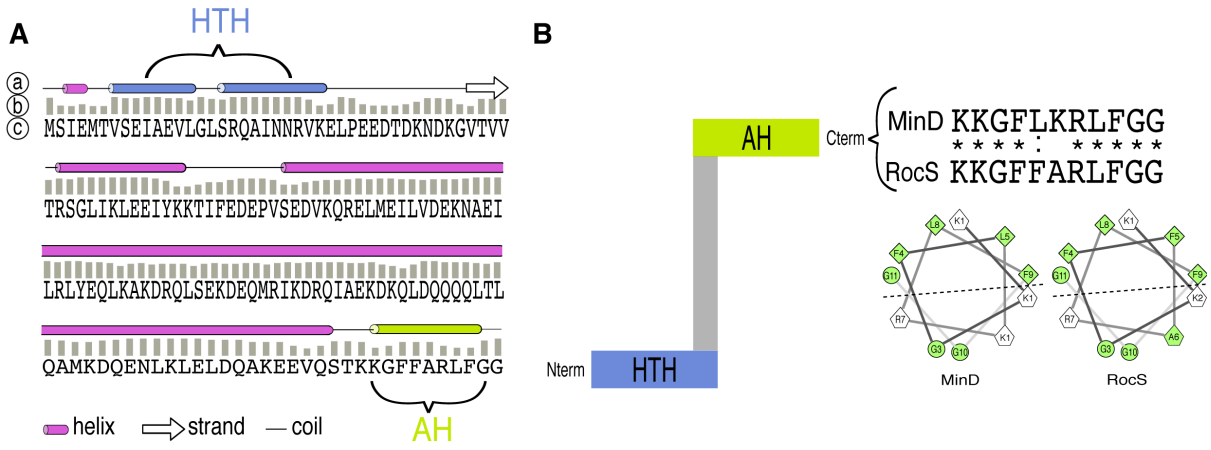

Figure S11: Growth curves and cell viability of *rocS*-Δ*AH* and Δ*HTH-rocS* mutants
(A) Growth curves of R800 (grey), Δ*rocS* cells (orange), *rocS*-Δ*AH* (green), or Δ*HTH-rocS* (dark blue) strains in CH+Y medium at 37 °C. The OD_{550} was read automatically every 10 min. (**B**) Histogram showing cell viability of the same strains. The color code is the same as in A. The experiment was performed in triplicates. Standard errors are indicated with error bars.

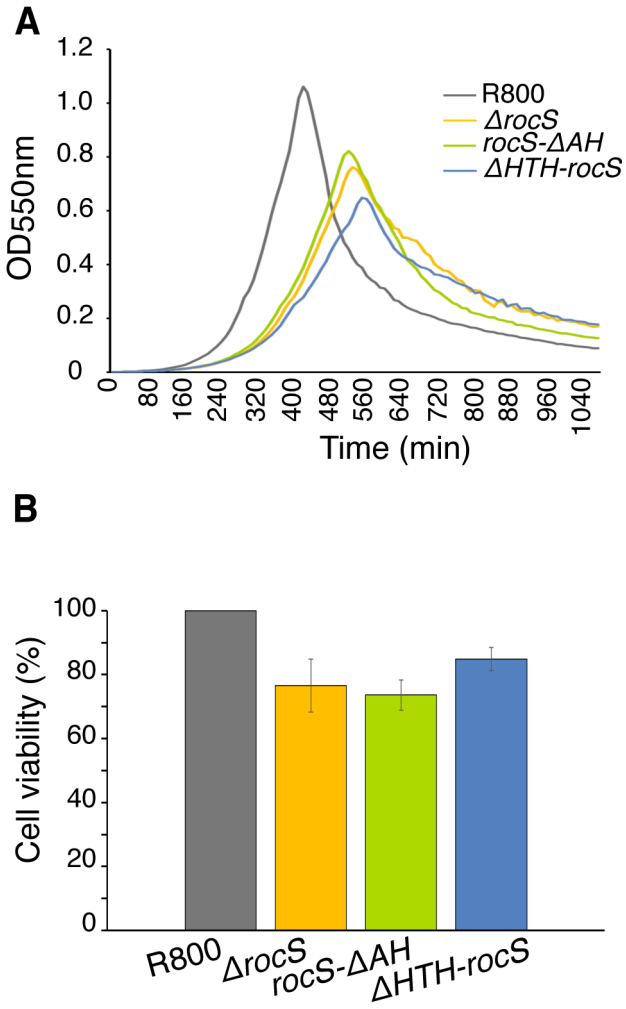

Figure S12: RocS directly interacts with the DNA *in vitro*
Electrophoretic mobility shift assays (EMSA) on agarose gels stained with ethidium bromide and developed under UV light. The indicated concentrations of purified RocS-ΔAH-6His were incubated with DNA fragments (50 ng) (**A**) of different lengths (50, 100, 200, 400 or 800 bp) and (**B**) GC contents (all fragments are 800 bp in length).

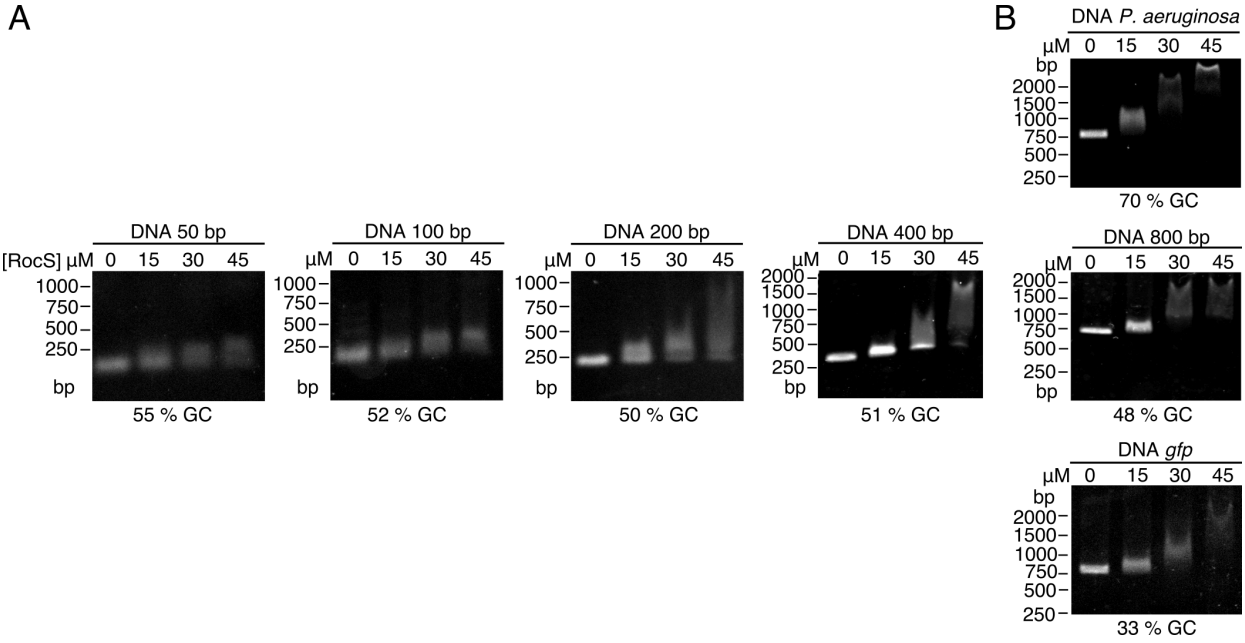

Figure S13: Interaction between RocS and ParB

(A) Immunoprecipitation of ParB-sfGFP (*10*) with FLAG-RocS in *flag-rocS-parB-sfgfp* and *flag-rocS* strains using anti-FLAG antibodies. Samples were analyzed by immunoblotting using either anti-FLAG antibodies (lower panel) to check that the same amount of RocS was loaded, or anti-GFP antibodies (upper panel) to determine the presence of co-immunoprecipitated ParB-sfGFP. (**B**) Protein purification. ParB and RocS-AH were overproduced in *E. coli* as 6His-tagged fusion proteins. After purification using a Ni-NTA resin, ParB-6His and RocS-ΔAH-6His were analyzed by SDS-PAGE. (**C**) Affinity measurements by Microscale Thermophoresis of labeled RocS binding to increasing concentrations of ParB-6His. FNorm (normalized fluorescence = fluorescence after thermophoresis / initial fluorescence) is reported on the y-axis and ligand concentrations on the x-axis are plotted in Molar. Measures are represented by blue dots and fitted curves by green lines. Three independent experiments were performed.

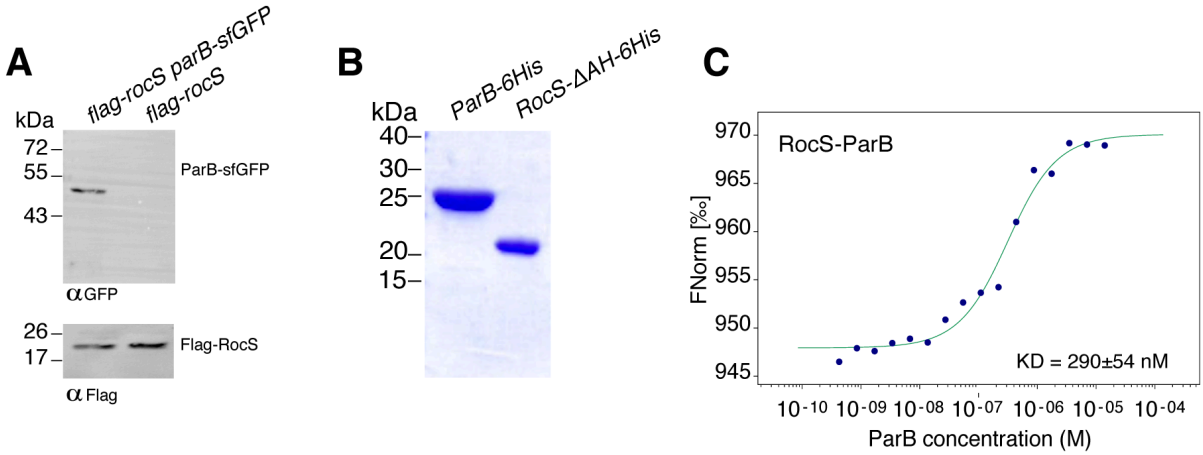

Table S1 : Strains and plasmids

Strains	Genotype and description	Reference	Primers
	S. pneumoniae strains		
R800	R800	23	
Δ rocS	R800 *rpsL::rpsL1; Δ rocS*	This study	5-6 ; 7-8
Δ rocS-P comX- rocS	) *rpsL::rpsL1; Δ rocS ; Δ IS1167::P1::P comR ::comR, cpsN-O::P comX ::r*	This study	9-10-11-12
Δ Nter-rocS	R800 *rpsL::rpsL1; rocS:: Δ nter-rocS*	This study	3-14-13-4
rocS- Δ Cter	R800 *rpsL::rpsL1; rocS::rocS Δ cter*	This study	3-15-16-4
gfp-rocS	*R800 rpsL::rpsL1; rocS::gfp-rocS*	This study	3-17-18-4
gfp- Δ Nter-rocS	R800 rpsL::rpsL1; rocS::gfpDnter-rocS	This study	3-17-19-4
gfp-rocS- Δ Cter	R800 rpsL::rpsL1; rocS::gfp-rocSDcter	This study	3-17-18-4
parB-sfgfp-spc	R800 rpsL::rpsL1; parB::parB-sfgfp-spec	This study	22-23
hlpa-mKate2	R800 *rpsL::rpsL1; hlpa::hlpa-mKate2-cm*	9	
hlpa-mKate2- Δ rocS	R800 *rpsL::rpsL1; hlpa::hlpa-mKate2-cm; Δ rocS*	This study	3-4
flag-rocS	R800 *rpsL::rpsL1* ; *rocS::FLAG-rocS*	This study	25-26
flag-rocS-parB-sfgfp-spc	R800 rpsL::rpsL1; rocS::FLAG-rocS; parB::parB-sfgfp-spc	This study	22-23
parS Ef	R800 *rpsL::rpsL1; thmA-IS1167 :: parS E.f*	This study	30-31
PcomX-repC-gfp	*R800 rpsL::rpsL1; DIS1167::P1::PcomR::comR; cpsN-O::PcomX::repC-gfp*	This study	10-12-28-29-36-37
parSEf PcomX-repC-gfp	*R800 rpsL::rpsL1; DIS1167::P1::PcomR::comR; cpsN-O::PcomX::repC-gfp; thmA-IS1167 :: parSE.f*	This study	9-28-29-12-30-31
DrocS parSEf PcomX-repC-gfp	*R800 rpsL::rpsL1; DrocS; DIS1167::P1::PcomR::comR; cpsN-O::PcomX::repC-gfp; thmA-IS1167 :: parSE.f*	This study	9-28-29-12-30-31
R800 *dnaA* TS	R800 *rpsL::rpsL1; dnaA ts*	This study	54-55
D39	virulent strain	10	
D39 *Δ rocS*	D39 *rpsL::rpsL1; Δ rocS*	This study	3-4
Δ rocS-P comX - rocS	D39 *rpsL::rpsL1; Δ rocS; Δ IS1167::P1::P comR ::comR; bbgA::P comX ::rocS*	This study	9-10-11-12
D39 Δ*cpsD*	D39 *rpsL::rpsL1; Δ* cpsD	10	
D39 *cpsD-3YF*	D39 *rpsL::rpsL1* ; cpsD::cpsD-3YF	10	
D39 *cpsD-3YF- Δ rocS*	D39 *rpsL::rpsL1* ; cpsD::cpsD-3YF; *Δ rocS*	This study	3-4
D39 *cpsD-3YE*	D39 *rpsL::rpsL1* ; cpsD::cpsD-3YE	10	
D39 *cpsD-3YE- Δ rocS*	D39 *rpsL::rpsL1* ; cpsD::cpsD-3YE; *Δ rocS*	This study	3-4
	***E. coli* strains**		
XL1-Blue	*supE44 hsdR17 recA1 endA1 gyrA46 thu relA1 lac - F'[proAB + lac] q lacZ Δ M15 Tn10 (Tc R)*	25	
BL21 (DE3)	F- *ompT gal dcm lon hsdS B (r B -m α -) λ (DE3 [lacI lacUV5-T7* gene *I indl sam7 nin5])*	26	
	Plasmids		
pT7.7	pT7.7 derivative, encoding a His-tag for C-terminal fusions	29	
pT7.7 *parB*	pT7.7 derivative, encoding *par,* from Met1 to Lys252	10	
pT7.7 *rocS Δ Cter*	pT7.7 derivative, encoding rocS, from Met1 to Gln150	This study	32-33
pQE30	pQE30 derivative, encodinf a *his-tag* for N-termal fusion	Qiagen	
pQE30 *cpsC/D* TIGR4	pQE30 derivative, encoding CpsD, from Met1 to Lys227, fused to the C-terminal part of CpsC, from Leu200 to Lys230	10	
pGBDU-C1	pGBDU derivative, encoding binding domain of *gal4* for N-terminal fusions, *ura3*	31	
pGBDU-C1-*cpsD*	pGBDU derivative, encoding *cpsD* , from Met1 to Lys226	10	
pGAD-C1	pGAD derivativ, encodind activation domain of *gal4* for N-terminal fusion, *leu2*	31	
pGAD-C1-*cpsD*	pGAD derivative, encoding *cpsD* , from Met1 to Lys226	10	

Table S2 : List of Primers

Forward and reverse primers are represented by plus (+) or minus (-), respectively

Number	Name	Sequence 5'-3'
1	Janus cassette (+)	CCGTTTGATTTTTAATGGATAATG
2	Janus cassette (-)	AGAGACCTGGGCCCCTTTCC
3	Upstream of *rocS (+) JPL1*	GTCTGCTATGAGTGTGGCGATTTTGGC
4	Dowstream of *rocS* (-) JPL4	CTACTTTCTGTCTCTAACAATTCCCTAG
5	Upstream of rocS / Janus (-)	CATTATCCATTAAAAATCAAACGGAATATCCTCTGAAACGTTTTCTAGC
6	Janus / Dowstream of rocS (+)	GGAAAGGGGCCCAGGTCTCTTCAAGGAGCTGTTTAGGTTAAATGC
7	ΔrocS (+)	TCAAGGAGCTGTTTAGGTTAAATGC
8	ΔrocS (-)	GCATTTAACCTAAACAGCTCCTTGAAATATCCTCTGAAACGTTTTCTAGC
9	*cpsN / rocS (+)*	ATTTATATTTATTATTGGAGGTTCAATGAGTATTGAAATGACC
10	*cpsN-O (-)*	TTTCTAATATGTAACTCTTCCCAAT
11	*rocS / P_{comX} (-)*	ATTGGGAAGAGTTACATATTAGAAATTATCCTCCAAATAAACGAGCAA
12	*$P_{comXS.ther}$ (+)*	TGAACCTCCAATAATAAATATAAAT
13	ΔNter-rocS (+)	GTTTCAGAGGATATTATGAGTATTGAATTACCAGAAGAAGACACAGATAAAAAT
14	ΔNter-rocS (-)	AATACTCTAAATATCCTCTGAAACGTTTTGACCTAG
15	rocS-ΔCter (+)	GCAAAAGAAGAAGTCCAATCCACTTAATCAAGGAGCTGTTTAGGTTAAATG
16	rocS-ΔCter (-)	AGTGGATTGGACTTCTTCTTTTGC
17	gfp-rocS (-)	CTTCACCTTTAGAAATCATAATATCCTCTGAAACGTTTTC
18	gfp-rocS (+)	CTCGAGGGATCCGGAATGAGTATTGAAATGACC
19	gfp-ΔNter-rocS (+)	CTCGAGGGATCCGGAATGAGTATTGAAATGACC
20	gfp (+)	AAACTAGACATCGAGTTCCTGCAGATGATTTCTAAAGGTGAAGAATTG
21	gfp (-)	TTATTTATACAATTCATCCATACC
22	Upstream of *parB* (+)	CTGACACTTTCTCTGATATTGC
23	Downstream of *parB* JN119 (-)	GGGATATATTTAACACGCGCATTAGG
24	Upstream of *hlpa* (+)	CGAAGTTAGCTCAAGAAG
25	Downstream of *hlpa* (-)	CAGGTTGATATTATCG
26	Flag-rocS (+)	GACTACAAAGACCATGACGGTGATTATAAAGATCATGATATCGACTACAAAGATGACGACGA TAAACTCGAGGGATCCGGAATGAGTATTGAAATGACC
27	Flag-rocS (-)	TCCGGATCCCTCGAGTTTATCGTCGTCATCTTTGTAGTCGATATCATGATCTTTATAATCACCG TCATGGTCTTTGTAGTCAATATCCTCTGAAACGTTTTC
28	cpsN / repC (+)	ATTTATATTTATTATTGGAGGTTCAATGAGTAAGTATACATTTC
29	*repC / P_{comX} (-)*	ATTGGGAAGAGTTACATATTAGAAATTATTTATACAATTCATC
30	parS E.f (+)	GTTCATTGTAAATACGGTTTAC
31	parS E.f (-)	CTTCCCAACGCCGCCTTTG
32	pT7-7 rocS (+)	TATCATATGGAAGACACAGATAAAAATGACAAAGGG
33	pT7-7 rocS (-)	TATCTGCAGTTAAGTGGATTGGACTTCTTCTTT
34	bggA (+)	GGTTTTGACTCTATCTCGCTTATTTAATTG
35	bggA (-)	GCCGGCTGTATCTACGATACC
36	repC E.f (+)	CCATTATTTTAACACACGAGGTGCTACCATGAGTAAGTTATACATTTCA
37	repC E.f (-)	CTGCAGGAACTCGATGTCTAGTTTTTTTTGTTTCTTTTTGTCTCG
38	DNA 50 pb (+)	TGTTGCCATTGCTACAG
39	DNA 50 pb (-)	GCCATACCAAACGACG
40	DNA 100 pb (+)	CGCCAGTTAATAGTTTGCG
41	DNA 100 pb (-)	TCGTTGGGAACCG
42	DNA 200 pb (+)	CGCCTCCATCCAGTCTATTAATTG
43	DNA 200 pb (-)	GAGCTAACCGCTTTTTTGCAC
44	DNA 400 pb (+)	CAATGATACCGCGAGACCCACG
45	DNA 400 pb (-)	TACGGATGGCATGACAGTAAG
46	DNA 800 pb (+)	CTAGATCCTTTTAAATTAAAAATG
47	DNA 800 pb (-)	TCGAACTGGATCTCAACAG
48	DNA *P.aeruginosa* (+)	GCTGGCCAGCCCGCGCGAGC
49	DNA P.aeruginosa (-)	GAACGGCTGCAGGTAGCTGAG
50	qPCR_parB (+)	ACGGTCTATCCCAGCTGTTG
51	qPCR_parB (-)	ATAGGCGCGTGCTTCTTCTA
52	qPCR_ter (+)	GAAAAGTACCATCCCCAGCA
53	qPCR_ter (-)	AGCCTTGGTGCCTATCATTG
54	dnaA forward	TAGAAGGGCTCGAGGAGAGG
55	dnaA reverse	CTTGCAGCAAAGGCTGTTTC

Movie S1: Nucleoid segregation in wild type R800 cells

Time-lapse analysis of HlpA-mKate2 in WT cells. The video shows an overlay of mKate2 (red) and phase-contrast (gray) images. Scale bar: 1μM. Time interval: 3 min.

Movie S2: Absence of chromosome segregation in Δ*rocS* cells

Time-lapse analysis of HlpA-mKate2 in Δ*rocS* cells. The video shows an overlay of mKate2 (red) and phase-contrast (gray) images. Scale bar: 1μM. Time interval: 3 min.

Movie S3: Chromosome pinching in Δ*rocS* cells

Time-lapse analysis of HlpA-mKate2 in Δ*rocS* cells. The video shows an overlay of mKate2 (red) and phase-contrast (gray) images. Scale bar: 1μM. Time interval: 3min.

Movie S4: Localization of GFP-RocS

Time-lapse analysis of GFP-RocS in wild-type cells. The video shows an overlay of GFP (green) and phase-contrast (gray) images. White head arrows highlight bright clusters that remain stationary for at least 3 consecutive frames. Scale bar: 1 μm. Time interval: 100 ms.